Studia Geotechnica et Mechanica, 2024; 46(4): 328–336

Original Study Open Access

Mikołaj Urbaniak*, Krzysztof Zamiar, Stanisław Kostecki

Understanding Geotechnical Embankment Washout Due to Overtopping: Insights From Physical Tests

https://doi.org/10.2478/sgem-2024-0025
received May 15, 2024; accepted October 6, 2024.

Abstract: Understanding the erosion process of an earth dam and flood embankment composed of noncohesive, homogeneous soils due to overflow is crucial for determining the quantity and rate of water release. This is necessary to assess the consequences of a failure, analyze the risk, and develop appropriate crisis management procedures. Despite numerous studies in this area, the process of breach evolution is not fully explored. The article presents the results of physical experiments carried out in the field laboratory of the Wrocław University of Science and Technology for a dam with a height of 0.50 m that closes a reservoir with a capacity of 14.4 m^3, whose width is significantly greater than the final width of the breach. The scenario analyzed assumes that water overflows the embankment crest, as it is the most common cause of embankment failure based on dam disaster databases. At the same time, the amount of water accumulated in the reservoir is the largest possible for this scenario, suggesting that such a catastrophe may have the most severe consequences. Based on the results obtained from three experiments, four repeatable phases of erosion evolution were identified and described: (I) the initiation phase, (II) the vertical erosion phase, (III) the lateral erosion phase, divided into two cycles, and (IV) the reservoir emptying phase without further propagation of the breach. The outflow rate of the water from the reservoir was also analyzed, allowing the determination of the outflow hydrograph for each test. Hydrographs showed differences between individual experiments; however, the average erosion rate was similar for all tests. Furthermore, the final width of the breach created each time was between 2.2 and 2.5 H (where H is the height of the embankment) and the volume of eroded soil ranged from 0.52 to 0.59 m^3. The article also highlights the methodology to calculate the water outflow hydrograph.

***Corresponding author: Mikołaj Urbaniak,** Wroclaw University of Science and Technology, Wroclaw, Poland, E-mail: mikolaj.urbaniak@pwr.edu.pl
Krzysztof Zamiar, Stanisław Kostecki, Wroclaw University of Science and Technology, Wroclaw, Poland

Keywords: dam safety, flood risk management, overtopping, embankment dam, laboratory tests, breach parameters, breach mechanism

1 Introduction

Research on water reservoir disasters is important due to their potential environmental, social, and economic consequences. According to Zhong et al. (2021), the water overflowing the crest of a reservoir dam accounts for 48% of all documented disasters, emphasizing the need to understand the erosion process of dams for this scenario. Precision recognition of the erosion process is crucial to assess the safety of areas downstream of the reservoir, as it allows the creation of flood hazard maps and evacuation plans based on the outflow hydrographs. Despite the increased financial and organizational resources needed to conduct laboratory studies, they provide not only an advanced tool for determining the evolution of the shape of the breach, but also a basis for validation and verification for modern numerical methods capable of analyzing this issue.

In recent years, experimental studies on homogeneous dams constructed of noncohesive soils eroded due to water overflowing the crest of the dam have been undertaken by many researchers. Coleman et al. (2002) conducted laboratory research and described the erosion process for homogeneous earth dams made of noncohesive soil with a height of 0.30 m while maintaining a constant water level in the upper reservoir. As a result of the water overflowing the dam crest, deep erosion is observed, which then transitions to lateral erosion, increasing the total width of the breach. Based on the results obtained, dimensionless relationships were proposed that describe the maximum flow through the breach and a methodology to predict the evolution of erosion in the horizontal and vertical directions. Based on the analysis of results from nine experiments, Chinnarasri et al. (2004) identified correlations of significant variables affecting the final parameters of breaches in homogeneous dams constructed of noncohesive soils. The authors indicated that the maximum intensity of outflow through

Open Access. © 2024 Mikołaj Urbaniak, Krzysztof Zamiar, Stanisław Kostecki, published by Sciendo. This work is licensed under the Creative Commons Attribution alone 4.0 License.

the breach is influenced not only by the characteristics of the reservoir (volume and depth of water in the reservoir), but also by the median grain size building the dam and the slope of the downstream slope. Asghari Tabrizi et al. (2017) conducted experiments on homogeneous dams with a height of 0.15 m, investigating the effect of soil compaction on the erosion process of the embankment. Based on the results obtained, two dimensionless equations were developed that describe the change in the height of the crest and the horizontal progress of erosion depending on the degree of compaction of the embankment. The dependencies obtained were consistent with the results observed from three small dam failures in South Carolina. Based on the analysis of 126 cases of earth dam failures and using nonlinear regression analysis, Ashraf et al. (2018) developed a new set of empirical equations to assess the effects of dam failures, including the width of the breach, the time of erosion of the breach, and the maximum flow from the breach. These relationships were validated in physical experiments by the authors on dams with heights of 0.90 and 1.80 m constructed from various types of soil. Empirical formulas for describing the basic parameters of catastrophic events have been developed by several researchers, including Soliman (2015) and Webby (1995). The formulas of Soliman (2015), derived from an analysis of 166 historical disasters, are applicable to both overtopping and piping failures. Webby (1995), utilizing a database of 22 disasters, formulated an equation specifically for estimating peak discharge. Abdellatif Mohamed & El-Ghorab (2016) investigated the influence of scale effects on the erosion process of homogeneous sand-built dams in experimental studies. After conducting experiments on dams with heights of 0.90 and 0.45 m and comparing them with the research by Ashraf et al. (2018), they concluded that there is a similarity in the erosion processes and rates of breach formation for large- and small-scale objects, suggesting that studies conducted on small-scale objects can be used to recognize the phenomenon of dam erosion. Orendorff et al. (2011) were the first to use particle tracking velocimetry (PTV) technology to measure the velocity of the water flow in the breach of an earth dam resulting from overflow of the crest of the dam. The research was carried out on dams with a height of 0.30 m. The application of PTV technology allowed for measurements of surface flow velocity through the breach, which reached a maximum value of 2.10 m/s. These results enabled the determination of breach geometry, that is, width and depth of flow. The obtained water depths were compared with the water depths determined on the basis of the analysis of the phenomenon, assuming a broad crest weir. Studies on determining erosion characteristics using large-scale particle image velocimetry (LSPIV) technology were continued by Bento et al. (2017). The authors proposed a method for determining the outflow hydrograph through the breach using a flow definition based on the product of the surface normal velocity and the estimated cross-sectional area of the breach. They used LSPIV technology to determine flow velocities. The proposed methodology was confirmed in laboratory studies on dams built with fine-grained materials. Kansoh et al. (2020) investigated the influence of shape parameters, such as slope of the downstream slope, crest width, and dam height, on the erosion process of homogeneous dams. Li et al. (2021) conducted research aimed at recognizing the erosion process for earth dams with a height of 0.60 m constructed of a sand–gravel mixture, taking into account seepage phenomena and the influence of drainage from the embankment on the evolution of dam erosion.

As the above description shows, the phenomenon of soil dam breaching is still not fully understood and described. The process depends on many parameters related to the material of the dam, the geometry, the size of the reservoir, and the initial conditions (initiating channel). We believe that our research on this topic provides crucial insights that can aid in the development and calibration of numerical models related to dam breach. This article presents the results of experimental studies concerning the erosion process of a homogeneous earth embankment with a height of 0.50 m closing a reservoir with a capacity of 14.4 m^3. The width of the test site did not restrict the width of the breach. The scenario examined during the three trials involves the overflow of water above the crest of the embankment as the cause of erosion. The inflow of water to the reservoir was stopped at the beginning of the experiment. The analysis focusses on the mechanism of breach formation and the characteristics of the outflow of water from the reservoir. Especially, we present a detailed mechanism of dam breach, highlighting four distinct phases of this process.

2 Description of the test site including a description of the test apparatus

The research in question was carried out in 2023 in the field laboratory of Wrocław University of Science and Technology. The laboratory is equipped with an underground water tank and a system of pumps and balancing tanks that supply the research stations in a closed circuit. To investigate the process of destroying a homogeneous geotechnical embankment due to overtopping, a setup was

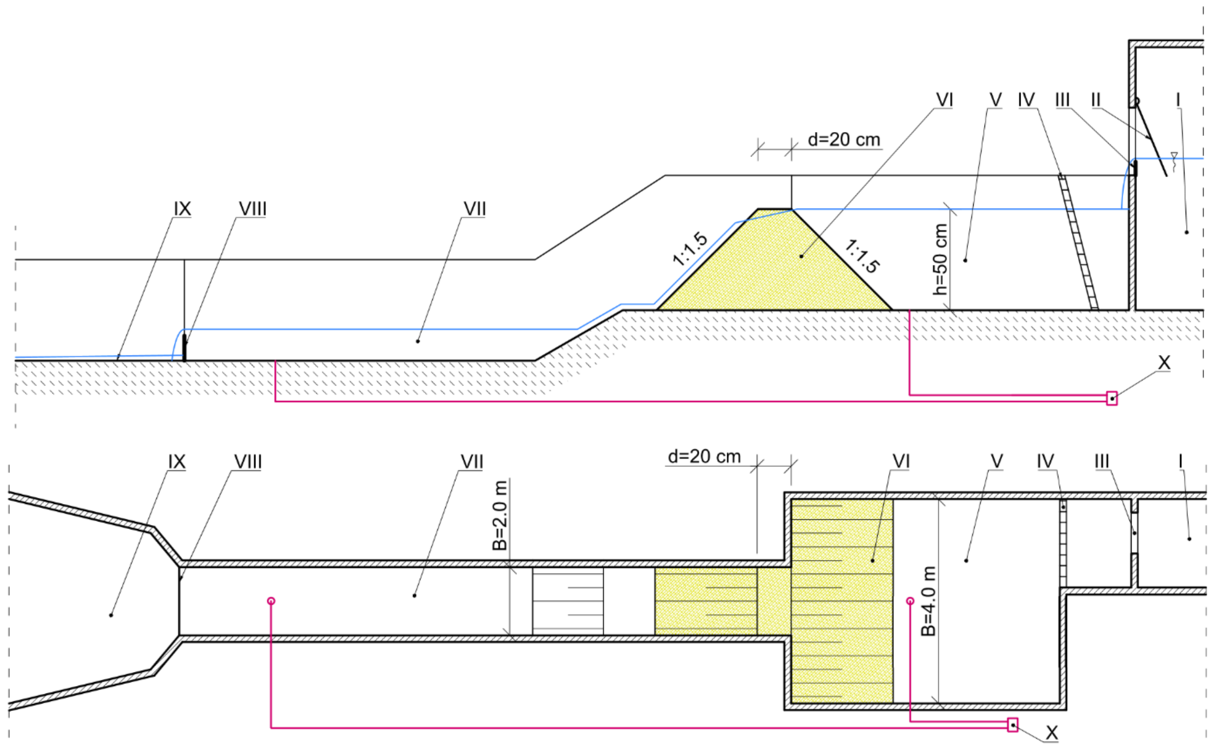

Figure 1: Experimental setup. I – balance tank, II – check valve (close of the overflow window), III – overflow window with Thomson's weir, IV – energy dissipation device, V – upper tank Vmax = 14.4 m3, VI – analyzed embankment, VII – downstream channel B=2.0 m, VIII – two Thomson's weirs, IX – free discharge channel B >> 2.0 m, X – hydrostatic pressure sensors.

constructed. It included a large upper tank with a capacity of 14.4 m^3 and a smaller drainage channel which ended with two Thomson's measuring weirs. Between the upper tank and the downstream channel, there is a base for an embankment. The embankment is 50 cm high, 200 cm long downstream, and 20 cm wide on the crest with a slope of 1:1.5. On the crest of the embankment, halfway along its length, a triangular erosion channel was created with a depth of 2.4 cm. A metal gutter with a foil apron was placed in the channel to protect the embankment from premature erosion initiation. Above the upper tank is a balancing tank that has an overflow window closed by a check valve (Fig. 1).

3 Measuring instruments

During the experiment, hydrostatic pressure was recorded at selected points using Keller's OEM series 11 sensors, with a measurement range of 0–1000 mm H_2O and an accuracy of approximately 0.01%–0.1%. In addition, survey rods and measuring strips were placed within the research setup. Four high-resolution video cameras were used to record the progression of erosion, determine the dimensions and propagation rate of the breach, and verify changes in water level. It allowed to conduct qualitative analysis of the data collected.

3.1 Description of the studies carried out

3.1.1 Embankment construction process

The construction of the embankment was carried out in layers, each with a thickness of 0.08 m. Each layer of the embankment was meticulously compacted using a 12-kg hand tamper dropped from a height of 0.15 m. This method ensured a consistent level of compaction in all the tests carried out, with a compaction index of I_s =0.90. The material used to build the embankment was sand, with an average particle size median of d_{50}=0.58 mm, and the grain size distribution curve of the soil used in each trial is presented below (Fig. 2). The Proctor parameters for this soil were a maximum dry density of 1.71 g/cm^3 and an optimum moisture content of 14%. Internal friction angle was 32°. For each test, the embankment was initially formed with larger plan dimensions and then precisely adjusted to the desired shape on the day of the experiment. For each test, the embankment construction process and the soil used were the same.

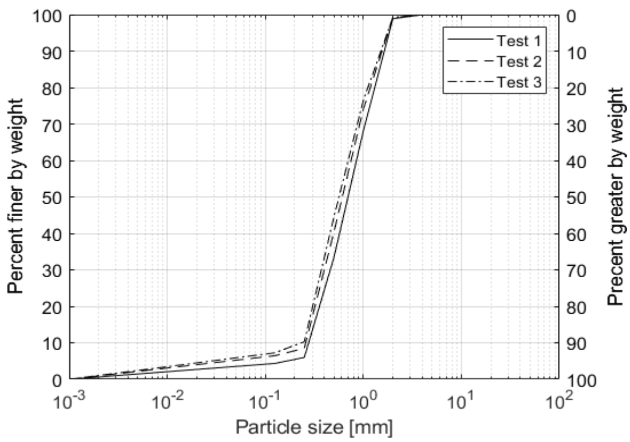

Figure 2: Distribution of grain size of the soil used in the laboratory test.

3.1.2 Experimental procedure

The experiments began by filling the drainage channel up to the level of the measuring weirs. The upper tank was then filled through the overflow window in the balancing tank. When the water level in the upper tank reached the bottom edge of the initiating erosion channel, the water inflow to the tank was cut off by closing the check valve in the balancing tank and the protective gutter was removed from the embankment, marking the start of the actual experiment. The accumulated water volume in the reservoir flowed freely down the embankment, eroding it and creating an expanding breach. As erosion progressed, the level of water in the drainage channel above the weirs changed.

In total, five trials were conducted, the first two serving as a learning experience for the experiment procedure. Measurements were taken in the following three trials. Each time, the embankment was reconstructed from scratch using the same construction technique, ensuring uniform initial parameters for each test.

4 Results and discussion

4.1 Breach erosion process

The research carried out revealed a four-phase dam erosion process, as depicted in Fig. 3. Phase I, the initiation phase, involves the flow through the initiating channel, generating minor erosion on the downstream face of the embankment, forming a small channel starting at the edge of the crest. When the water stream creates a channel on the slope surface that reaches the toe of the dam, phase II begins, where backward erosion plays a crucial role, eroding the embankment from the downstream face toward the reservoir, opposite to the direction of water flow. The pace of this process is dependent on the velocity of water flowing through the breach. As the breach deepens, the stream flows with increasing velocity, causing accelerated erosion of the soil in the lower parts of the embankment and undermining the side walls of the formed gap. As a result, the stability of the side slope fragments decreases, eventually leading to the detachment of soil chocks. When the first fragment is detached from the dam crest, the most dangerous phase III, the lateral erosion phase, begins. During this phase, two repeating cycles are visible. Cycle IIIa involves the erosion of the dam in a direction perpendicular to the direction of water flow. The stream of water hitting the base of the dam disperses sideways; however, due to the presence of the dam walls, a helical vortex with a horizontal axis is formed. As a result, the water “bites into” the sidewall, creating an increasingly overhanging structure. At some point, the overhang loses stability, initiating cycle IIIb, during which the previously undercut soil mass detaches from the embankment, dramatically widening the upper edge of the overflow and falling into the water stream. For a short period, the water stream erodes the detached soil mass until it is completely removed from the gap area, marking the beginning of another cycle IIIa. With the consistent widening of the overflow crest, the amount of water flowing through the breach increases, further enhancing backward erosion and lowering the bottom of the breach, which represents the weir crest. As the level of water in the reservoir decreases due to the outflow through the breach, the energy of the outflowing stream decreases, slowing the erosion until the lateral erosion ceases. With the detachment of the last soil wedge, the final phase, the reservoir emptying phase, is identified. In this phase, the remaining water in the reservoir flows out with almost constant breach dimensions. Erosion in this phase is minimal and mainly concerns backward erosion. The duration of each phase for each trial is presented in Fig. 4. The most varied is the duration of phase I, while phase II is the most repeatable, with durations ranging between 33 and 38 s.

4.2 Breach width and outflow

Fig. 5 depicts the change in the width of the breach during phase III, the lateral erosion phase, where the release of water is at its highest. Segments with constant values represent cycle IIIa, which involved undercutting

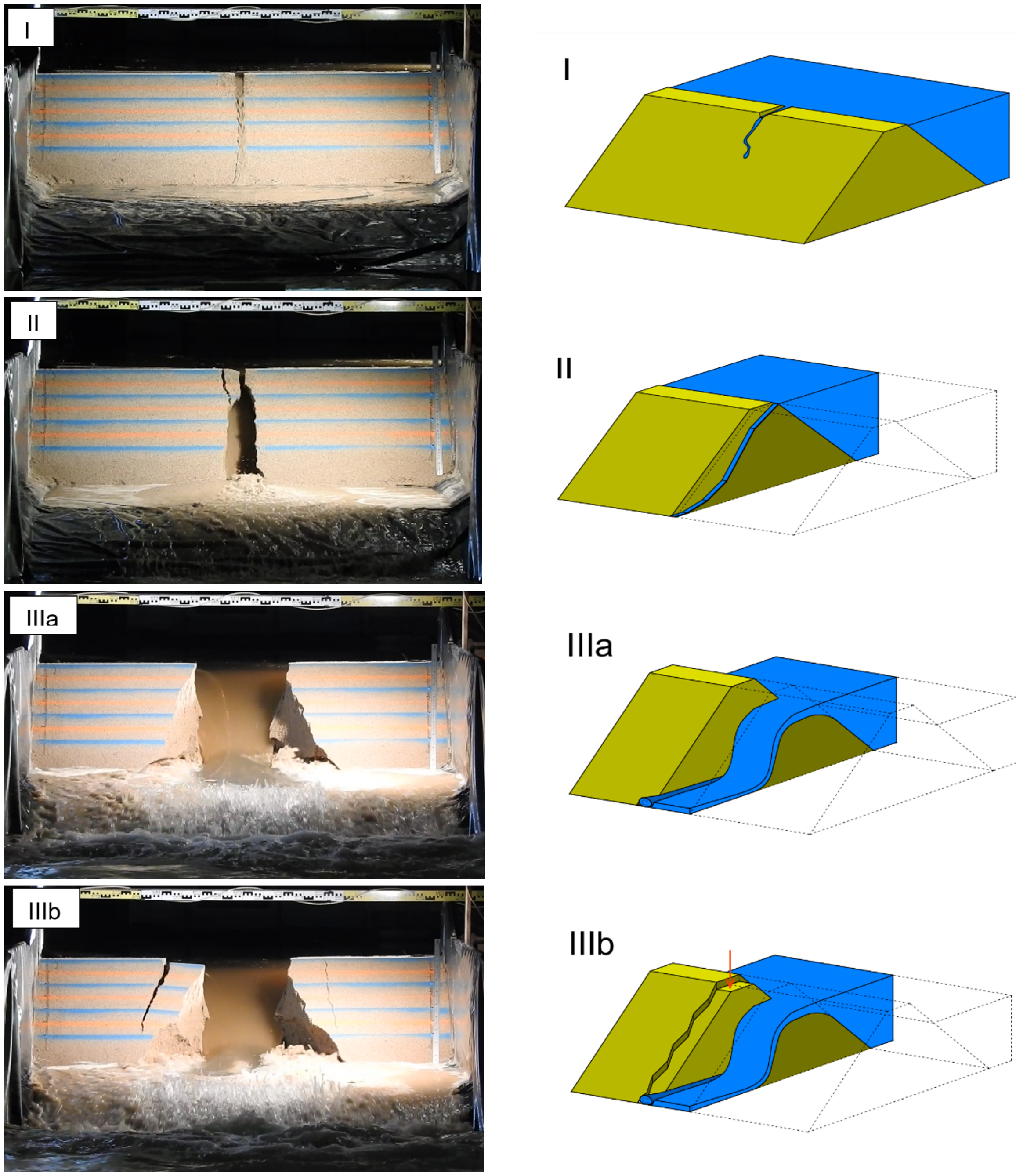

Figure 3: Phases of failure mode of a noncohesive homogeneous dam – photos from Test 2 and isometric schemes.

the base of the embankment without visible effects on the crest of the dam. Sudden jumps in the values on the graph indicate moments when additional soil masses detached, initiating cycle IIIb of phase III. The results obtained for Test 1 and Test 2 show similarity in the increase in the width of the breach measured on the crest of the embankment, indicating that the subsequent soil masses detached within similar time intervals. The final breach width was reached at 89 and 76 s for Test 1 and Test 2, respectively, from the beginning of phase III. Test 3 significantly deviates from the results obtained for the previous two trials; in this case, the final width of the breach was reached in 46 s, indicating a significantly faster lateral erosion process. In addition to the width of the breach, the water flow from the upper tank through the breach was also analyzed using water level recording probes. The course of each experiment was recorded and subjected to analysis. The basic method of determining

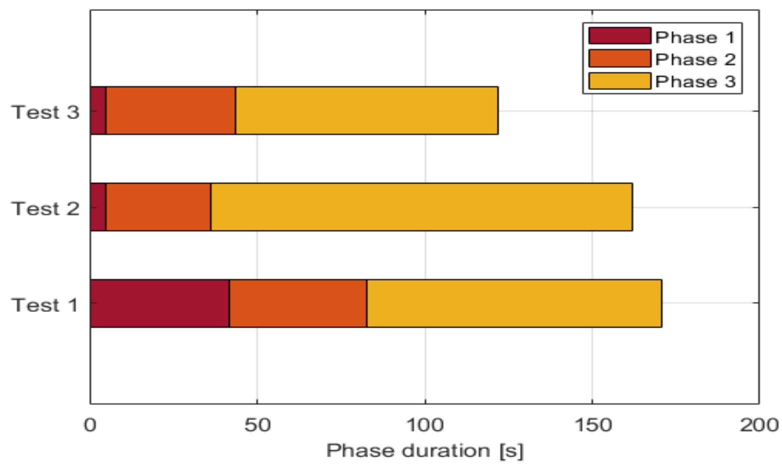

Figure 4: Phase duration in each test

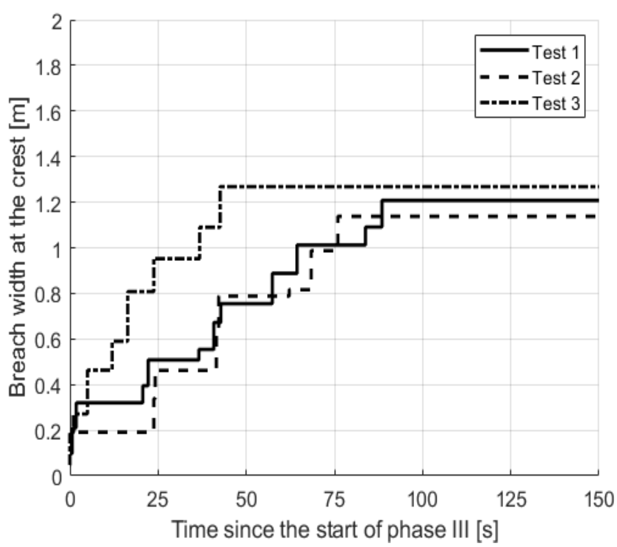

Figure 5: Breach width at the crest since the beginning of phase III.

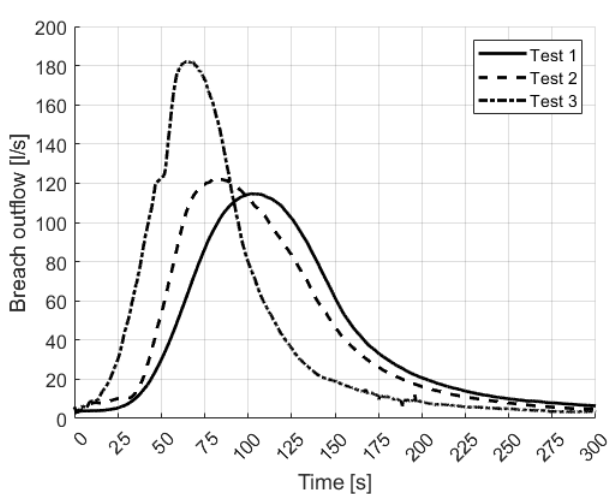

Figure 6: Upstream discharge from tests 1, 2, and 3.

the water outflow hydrograph through the breach involved determining the change in water volume in the upper tank over time when this change occurred. Fig. 6 presents the hydrographs computed from the three consecutive trials.

The upstream hydrograph was determined according to the methodology described above, while the downstream hydrograph was established using Thomson weir flow measurement devices located 9 m downstream from the centerline of the tested embankment (element VIII, Fig. 1). Upstream and downstream hydrographs and the water level in the reservoir for each test are shown in Figs 7–9. In Test 1, the increase in outflow intensity through the breach lasted 102 s, with the maximum outflow from the tank recorded at 102 s, reaching 114.65 l/s. In Test 2, the increase in outflow intensity through the breach lasted about 86 s and peaked at 122.67 l/s. The results of Test 3 differed from the results of the previous two experiments. The outflow intensity from the tank increased for approximately 64 s and reached a maximum value of 182.17 l/s. The results presented in Figs 5 and 6 also demonstrate similarity in the phenomenon in tests 1 and 2 and a difference in Test 3. Despite the differences indicated in the three trials, the final widths of the breach were similar and amounted to 1.21, 1.14, and 1.27 m, respectively; consequently, the amounts of eroded material were similar.

All the parameters determined from the embankment breach are presented in Tab. 1. The duration of erosion was measured from the beginning of phase I to the beginning of phase IV. The average erosion rate and the average lateral erosion rate were measured during phases II and III.

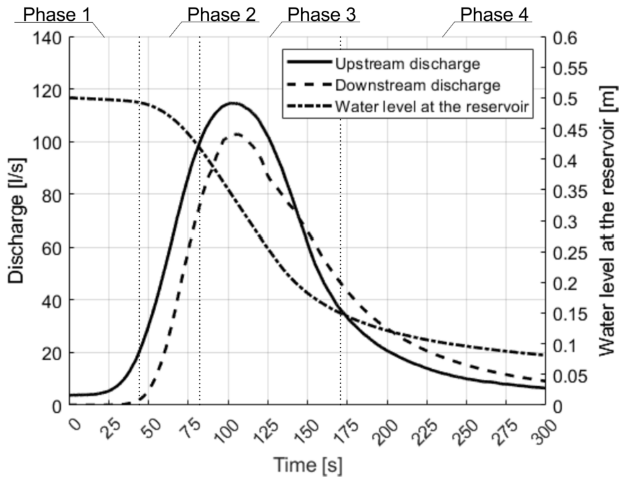

Figure 7: Discharge and water level from Test 1.

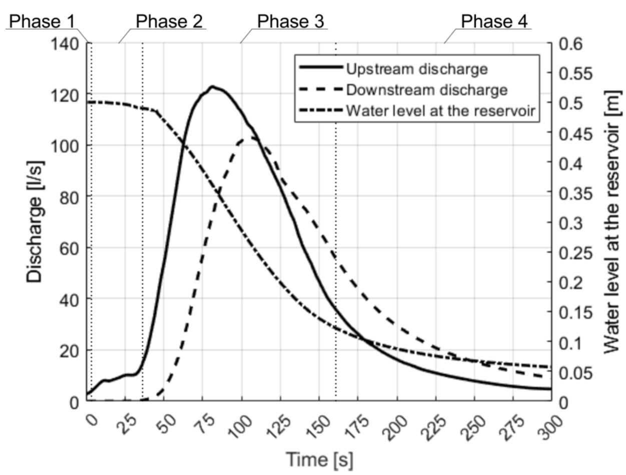

Figure 8: Discharge and water level from Test 2.

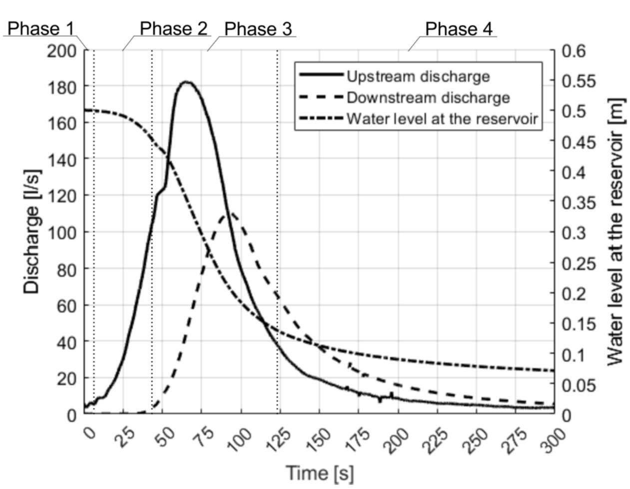

Figure 9: Discharge and water level from Test 3.

4.3 Comparison of the results with known formulae from other researchers

The results obtained have been compared with few empirical formulae (mainly those presented in Zhong et al. (2021), but not only) and in this paper, the authors focused on the values calculated using four empirical methods selected as the most appropriate in at least one parameter presented in Ashraf et al. (2018) Eq. (1); Webby (1995) Eq. (2); Chinnarasri et al. (2004) Eq. (3); and Soliman (2015) Eq. (4), describing the effects of embankment failure as a result of water overtopping the dam crest.

$$Q_p=127.3H^{0.6313}V^{0.7637} \tag{1a}$$

$$B_{avg}=13.197H^{0.4757}V^{0.1785} \tag{1b}$$

$$H_f=0.9067H^{1.0118}V^{0.013} \tag{1c}$$

$$T_f=5.935H^{-0.9499}V^{0.4135} \tag{1d}$$

$$Q_p = 0.0443 \cdot \left(\frac{H}{V^{\frac{1}{3}}}\right)^{1,4} \cdot \sqrt{gV^{\frac{5}{3}}} \tag{2}$$

$$Q_{p,\min} = 0.209 \cdot \left(\frac{H}{V^{\frac{1}{3}}}\right)^{1.613} \cdot \sqrt{gV^{\frac{5}{3}}} \tag{3a}$$

$$Q_{p,\max} = 0.020 \cdot \left(\frac{H}{V^{\frac{1}{3}}}\right)^{1.714} \cdot \sqrt{gV^{\frac{5}{3}}} \tag{3b}$$

$T_f=5.84V^{0.75}H^{0.76}Q^{-1}_{p,min/max}$, where $Q_{p,min/max}$ means $Q_{p,min}$ or $Q_{p,max}$ for $T_{f,min}$ or $T_{f,max}$, respectively. (3c)

$$B_{avg}=48.644\bullet V^{0.275}\bullet W^{-0.086} \tag{4a}$$

$$H_f=1.093\bullet H^{0.894}\ V^{0.027} \tag{4b}$$

$$T_f=0.15+1.865\bullet H^{-0.675}\ V^{0.408} \tag{4c}$$

where Q_p – peak flow (m³/s), B_{avg} – average breach width (m), H_f – breach height (m), T_f – breach formation time (h), H – dam height (m), W – dam length (m), V – reservoir volume (mln m³), and g=9.81 m/s – gravitational acceleration. In equation 3c, $Q_{p,min}/Q_{p,max}$ means $Q_{p,min}$ or $Q_{p,max}$.

From the empirical formulas proposed by Ashraf et al. (2018), the relationship describing the average width of the breach closely matches the results of the experimental studies conducted. The relationship proposed by Webby (1995) provides a good estimate of the maximum water outflow through the breach compared to the results obtained. Individual researchers have developed formulas that produce significantly different results. Even within the

Table 1: Dam breach parameters of tests 1, 2, and 3.

Test	Peak discharge (l/s)	Timing of the peak discharge (s)	Duration of breach (s)	Duration of expansion of the breach (s)	Eroded material (m^3)	Average erosion rate (m^3/s)	Final width of the top of the breach (cm)	Average rate of breach expansion (cm/s)
1	114.65	102	171	129	0.571	0.004	121	0.9
2	122.67	86	162	157	0.520	0.003	114	0.7
3	182.17	64	122	117	0.586	0.005	127	1.1

Table 2: Comparison of breach parameters using empirical formulas.

	Ashraf et al. (2018)	Soliman (2015)	Webby (1995)	Chinnarasri et al. (2004)	The present study		
					Test 1	Test 2	Test 3
Qp (l/s)	16.51	-	138.93	38.42/471.07*	114.65	122.67	182.17
B_{avg} (m)	1.30	2.41	-	-	1.20	1.10	1.23
Hf (m)	0.39	0.44	-	-	0.5	0.5	0.5
Tf (s)	411	654	-	75/79*	128	157	117

*The relationships determine the minimum and maximum possible values describing the erosion characteristics

scope of these experiments, despite identical experimental conditions, only two trials yielded consistent results. The maximum outflow from the reservoir in the third trial is noticeably different, yet all obtained results fall within the ranges specified by Chinnarasri et al. (2004).

5 Conclusions

This paper presents the results and analysis of an experimental study on the washing out of a homogeneous earth embankment made of noncohesive soil. Careful recording of the embankment breach process allowed to distinguish four repetitive erosion phases, which included the initiation phase, the vertical erosion phase, the lateral erosion phase, and the reservoir emptying phase. The observations made regarding the complexity of the lateral erosion phase, which includes the undercutting of the embankment footing and is followed by the detachment of chocks of soil, are in agreement with those described by Coleman et al. (2002), as well as those described by Chinnarasri et al. (2004). Of the three experiments conducted, two yielded similar results, while the erosion of the embankment in Test 3 was faster, resulting in a more intense outflow of water from the reservoir and a higher peak flow through the breach. All three tests resulted in a breach with very similar final parameters, suggesting that the geometric parameters of the breach depend less on the rate of the phenomenon and more on the amount of water stored in the reservoir. Analysis of the results suggests a correlation between the amount of energy stored in the reservoir and the amount of eroded material. In the next step of the laboratory study, it would be necessary to identify the reason why the results of Test 3 differed from the two preceding trials. A potential reason could be that the three tests generated two minimum and one maximum result for the scenario; however, the authors suspect that the difference in results may be due to the clay fraction content of the soil, which is difficult to determine during sieve analysis. These conclusions point to the need to perform physical tests, assuming a repeatable scenario. In addition, it is important to highlight the differences in the hydrographs upstream and downstream obtained by different methods. In Figs 7–9, clear differences can be seen between the results obtained from the change in the volume of water in the reservoir and those obtained from the flow through Thomson's weirs. The results obtained from the Thomson overflows indicate a lower maximum flow than those derived from the analysis of the reservoir emptying rate. The time difference between the occurrence of peak flows in the two methodologies is also noticeable. The reason for this is the capacity of the outflow channel that causes wave transformations. This shows how important it is for the presented studies to accurately describe the method of obtaining hydrographs, which can then be used for flood risk analysis. A comparison of laboratory results obtained for a small-scale dam to the results of calculations based on empirical formulas obtained from the analysis of real-scale dam disasters shows differences. It can be noted that the selected formulas fit the results f physical tests, for example, the maximum flow *Qp* according to Webby (1995) Eq. (2) or the average width of the breach B_{avg} according to Ashraf et al. (2018) Eq. (1) However, others deviate significantly from the results of laboratory studies, that is, time of failure *Tf* according to Ashraf et al. (2018) Eq. (1) or according to Soliman (2015) Eq. (3). The use of empirical formulae developed through statistical analysis of specific databases may be subject to some degree of inaccuracy due to limitations in the range of data used. This is particularly important in extremum cases, such as small-scale models. This means that it is difficult to estimate the behavior of experiments at the design stage, and that preliminary studies such as these are necessary for further research.

References

[1] Abdellatif Mohamed, M. M., & El-Ghorab, E. A. S. (2016). Investigating scale effects on breach evolution of overtopped sand embankments. *Water Science*, *30*(2), 84–95. https://doi.org/10.1016/j.wsj.2016.10.003

[2] Asghari Tabrizi, A., Elalfy, E., Elkholy, M., Chaudhry, M. H., & Imran, J. (2017). Effects of compaction on embankment breach due to overtopping. *Journal of Hydraulic Research*, *55*(2), 236–247. https://doi.org/10.1080/00221686.2016.1238014

[3] Ashraf, M., Soliman, A. H., El-Ghorab, E., & Zawahry, A. El. (2018). Assessment of embankment dams breaching using large scale physical modeling and statistical methods. *Water Science*, *32*(2), 362–379. https://doi.org/10.1016/j.wsj.2018.05.002

[4] Bento, A. M., Amaral, S., Viseu, T., Cardoso, R., & Ferreira, R. M. L. (2017). Direct Estimate of the Breach Hydrograph of an Overtopped Earth Dam*, 143 (6)*. https://doi.org/10.1061/(ASCE)HY.1943-7900.000129

[5] Chinnarasri, C., Jirakitlerd, S., & Wongwises, S. (2004). Embankment dam breach and its outflow characteristics. *Civil Engineering and Environmental Systems*, *21*(4), 247–264. https://doi.org/10.1080/10286600412331328622

[6] Coleman, S. E., Andrews, D. P., & Webby, M. G. (2002). *Overtopping Breaching of Noncohesive Homogeneous Embankments*. https://doi.org/10.1061/ASCE0733-94292002128:9829

[7] Kansoh, R. M., Elkholy, M., & Abo-Zaid, G. (2020). Effect of Shape Parameters on Failure of Earthen Embankment due to Overtopping. *KSCE Journal of Civil Engineering*, *24*(5), 1476–1485. https://doi.org/10.1007/s12205-020-1107-x

[8] Li, Y., Tian, C., Wen, L., Chen, A., Wang, L., Qiu, W., & Zhou, H. (2021). A study of the overtopping breach of a sand-gravel embankment dam using experimental models. *Engineering Failure Analysis*, *124*. https://doi.org/10.1016/j.engfailanal.2021.105360

[9] Orendorff, B., Rennie, C. D., & Nistor, I. (2011). Using PTV through an embankment breach channel. *Journal of Hydro-Environment Research*, *5*(4), 277–287. https://doi.org/10.1016/j.jher.2010.12.003

[10] Soliman, A. (2015). Hydrological Impacts of Renaissance Dam Failure on the Downstream up to the High Awan Dam, Ph.D Thesis. Faculty of Engineering, Cairo University, Giza, Egypt.

[11] Webby, M.G. (1995). Discussion of „Peak outflow from breached embankment dam". Journal of Water Resources Planning and Management, 1996, 122(4), 316-317.

[12] Zhong, Q., Wang, L., Chen, S., Chen, Z., Shan, Y., Zhang, Q., Ren, Q., Mei, S., Jiang, J., Hu, L., & Liu, J. (2021). Breaches of embankment and landslide dams - State of the art review. In *Earth-Science Reviews* (Vol. 216). Elsevier B.V. https://doi.org/10.1016/j.earscirev.2021.103597